

FSR 1735 – A new globular cluster candidate in the inner Galaxy

D. Froebrich^{1*}†, H. Meusinger² and A. Scholz^{3,4}

¹ Centre for Astrophysics and Planetary Science, University of Kent, Canterbury, CT2 7NH, UK

² Thüringer Landessternwarte Tautenburg, Sternwarte 5, 07778 Tautenburg, Germany

³ University of St. Andrews, Department of Physics & Astronomy, North Haugh, St. Andrews, Fife, KY16 8SS, Scotland, UK

⁴ University of Toronto, Department Astronomy & Astrophysics, 50 St. George Street, Toronto, Ontario M5S 3H8, Canada

Received sooner; accepted later

ABSTRACT

We carry out a large program to classify newly discovered star clusters from Froebrich et al. (2006) in the inner Galaxy. Here, we present a first analysis of a new high-priority globular cluster candidate, FSR 1735 at $l=339.1879$; $b = -1.8534$, based on new deep near infrared observations from Sofi at the NTT. A significant peak in the K-band luminosity function is found, which is interpreted as the clump of post-He-flash stars. The distance and the reddening of the cluster are determined to 9.1 kpc and $A_K=0.5$ mag, respectively, the metallicity is estimated to $[M/H]=-0.8$. Radial star density profiles are used to measure the core radius and the tidal radius of the cluster. The lack of signs for on-going star formation and the position in the Galaxy pose strong arguments against the interpretation of this object as a young or old open cluster. All the observational evidence is in agreement with the interpretation that FSR 1735 is a so far unknown globular cluster in the inner Galaxy.

Key words: Galaxy: globular clusters: individual

1 INTRODUCTION

Star clusters provide us with unique laboratory conditions to investigate various aspects of astrophysics. They represent groups of stars with similar ages, metallicities and distances. Beside testing stellar evolutionary models they also enable us to trace the distribution of interstellar material along the line of sight. Orbits of star clusters around the Galactic centre can be used to probe the distribution of mass in the Galaxy. Galactic open clusters (OCs) trace the recent star formation history in the Galaxy, while globular clusters (GCs) can be used to gather information about the formation and early evolution of the Milky Way. The differences in the formation of these cluster types is reflected in the distribution on the sky. While OCs are mainly distributed in the Galactic plane, GCs are concentrated towards the Galactic centre.

The number of known OCs has risen dramatically in recent years with the availability of deep large scale near infrared surveys such as 2MASS (Skrutskie et al. (2006)). Numerous surveys in the 2MASS catalogue were conducted to identify new star clusters (e.g. Carpenter et al.(2000); Dutra & Bica (2000),(2001); Ivanov et al. (2002); Bica et al. (2003); Kronberger et al. (2006); Froebrich et al. (2006)). Several hundred new clusters and cluster candidates were identified by these works, preferably close to the Galactic plane.

Contrary to OCs, the total number of known Milky Way GCs has increased by just a few percent over the last 25 years. So

far 152 Milky Way GCs are known, but this sample is very likely not complete. The "Catalog of Parameters for Globular Clusters in the Milky Way" by Harris (1996) lists 147 objects. In recent years, this sample was enlarged by five (perhaps six) objects: 2MASS GC01/02 (Hurt et al. (2000)); ESO 280-SC06 (Ortolani et al. (2000)); GLIMPSE-C01 (Kobulnicky et al. (2005)); GC Whiting1 (Carraro et al. (2005)); and perhaps SDSS J1049+5103 (Willman et al. (2005)). Originally most of the Milky Way GCs were discovered by visual inspection of photographic plates obtained at optical wavelengths. Close to the Galactic plane, however, many objects remained undiscovered due to obscuration from dust. This area, well known as the 'Zone of Avoidance' in extragalactic astronomy, might have a number of so far unknown Milky Way GCs in store. Based on the spatial distribution of the known GCs Ivanov et al. (2005) estimate a lower limit of 10 ± 3 unknown GCs near the Galactic plane ($|z| \leq 0.5$ kpc) and within 3 kpc from the Galactic centre. The Zone of Avoidance is obviously expected to be the least complete area in the Milky Way GC sample, though the recent serendipitous discoveries of the two off-plane clusters GC Whiting1 (Carraro et al. (2005)) and ESO 280-SC06 (Ortolani et al. (2000)) have demonstrated that the previous sample of off-plane clusters was also incomplete.

We are currently conducting a survey of star cluster candidates (selected from Froebrich et al. (2006)) to identify a substantial fraction of the missing Milky Way GCs in the Zone of Avoidance and to determine their properties such as distance, size, extinction, metallicity and age, based on deep NIR photometry. Here we present the observations of a first very promising new GC candidate un-

* Based on observations collected at ESO, Chile; ESO 077.B-0074(A)

† E-mail: df@star.kent.ac.uk

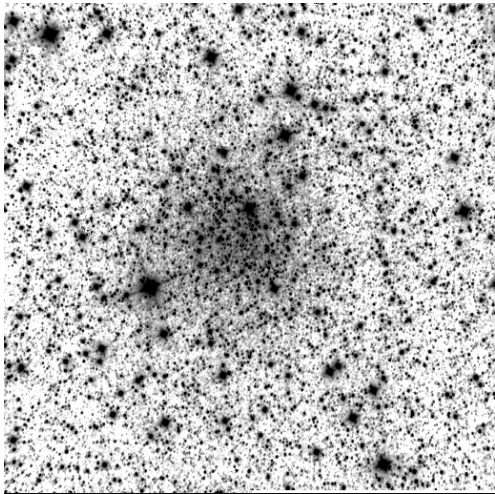


Figure 1. Logarithmic gray scale image of the cluster FSR 1735. The image size is $4.9' \times 4.9'$. North is to the top and East to the left.

covered by this survey. The cluster has the number 1735 in the list of Froeblich et al. (2006) and we will hence refer to the object as FSR 1735. Its accurate position is $l=339.1879$; $b=-1.8534$ or $\alpha = 16^{\text{h}}52^{\text{m}}10.6^{\text{s}}$, $\delta = -47^{\circ}03'29''$ (J2000), about half an arcminute south of the position given in Froeblich et al. (2006).

The paper is structured as follows. In Sect. 2 we present our data, followed by the determination of the properties of the star cluster in Sect. 3. This is followed by a discussion of the classification of the cluster in Sect. 4 and the conclusions.

2 DATA

As part of a larger program to study selected cluster candidates from Froeblich et al. (2006) in the Zone of Avoidance, observations with Sofi at the NTT were carried out on the 7th of May in 2006. We observed in Large Field mode with a pixel size of $0.288''$ and a field of view of $4.9' \times 4.9'$. In each of the three broad band filters (JHK_s) a total per pixel integration time of 225 s was achieved with short 5×5 s exposures. Standard procedures were used for flat-fielding, sky-subtraction and mosaicing.

The seeing in the co-added mosaics is $0.85''$. Source detection and photometry in the images was done using the SExtractor software (Bertin & Arnouts (1996)). Only objects that are detected above the three sigma noise level in all three filters are used in the subsequent analysis. Conditions were photometric and photometric calibration of the images was done using the variety of about 500 2MASS sources in the field around the cluster. The completeness limits (determined as the peak in the luminosity function) outside the cluster area are 18.1, 17.1, and 16.7 mag for JHK, respectively. Near the cluster centre we are much more hampered by source confusion and the completeness limits are 17.2, 16.3, 15.7 mag for JHK, respectively. Typical photometric errors for the latter brightnesses are 0.045, 0.047, 0.041 mag for JHK, respectively.

3 RESULTS

3.1 Basic properties

Our new deep JHK images show that the nebulous appearance of the cluster in 2MASS images is due to a large number of faint un-

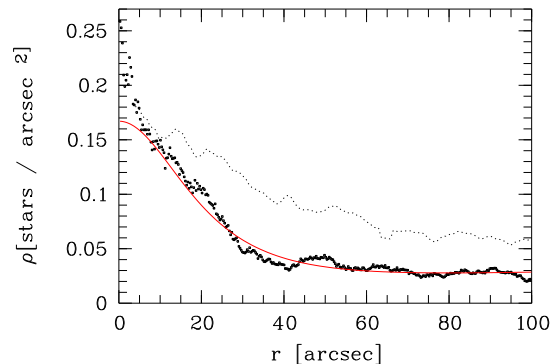


Figure 2. Observed K-band star density profile (dots) and best fitting King-profile (solid line) of the cluster. Overplotted as dotted line is the star density profile of the unresolved cluster population in arbitrary units.

resolved stars. In Fig. 1 we show the logarithmic gray-scale version of the K-band image of the cluster. The large number of stars in the cluster compared to the surrounding field can immediately be seen, as well as its almost circular appearance.

We determined the radial density profile of stars one magnitude above the local completeness limit in the cluster area (i.e. at $m_K = 14.7$ mag). This ensures that we are not too hampered by a possibly lower completeness limit in the very centre of the cluster. The resulting star density profile in Fig. 2 shows that a high number of bright stars is concentrated towards the centre of the cluster (note that the measured profile is smoothed with a $4.3''$ radius). The star density follows a King profile, with the best fit parameters: $R_{core} = 23.5''$, $R_{tid} = 86''$, $I_{cen} = 0.27^{**}/\text{arcsec}^2$, $I_{back} = 0.0278^{**}/\text{arcsec}^2$. Integrating the King profile till the tidal radius results in about 300 stars brighter than $m_K=14.7$ mag in the cluster. Only inside $4''$ from the centre the star density exceeds the King profile due to three bright stars around the central position.

We determined the radial profile of the average flux per pixel of the unresolved cluster population of stars by masking all detected stars. This profile is overplotted in arbitrary units as dotted line in Fig. 2. One can interpret this as the number of unresolved stars per pixel, i.e. the density of faint stars in the cluster. Hence, Fig. 2 allows us to compare the star density profile of the bright and faint stars in the cluster. From a King profile fit we determine $R_{core} = 41.5''$ and $R_{tid} = 125''$ for the unresolved stars. The apparent difference cannot be interpreted in terms of mass segregation due to the small difference in mass between giant - subgiant stars and (upper) main sequence stars. It has to be attributed to magnitude migration from faint to bright stars due to the significant crowding (larger than 30% in the inner $10''$) even at those bright magnitudes.

3.2 Reddening

We constructed colour-colour diagrams of the investigated area. Using only stars more than $100''$ away from the cluster centre (control field), we clearly identify two groups of objects: 1) stars with $H - K=0.27$ mag, $J - H=0.67$ mag, and $J - K=1.00$ mag, which represent almost unreddened foreground stars, mostly K- and M-dwarfs. 2) Objects with redder colours, which represent mostly reddened background giant stars. The gap in the colour-colour diagram between the two groups seems to indicate that one single cloud is responsible for most of the reddening in the field. The MSX Band A ($6-11 \mu\text{m}$) image indeed shows a faint cloud extending across our

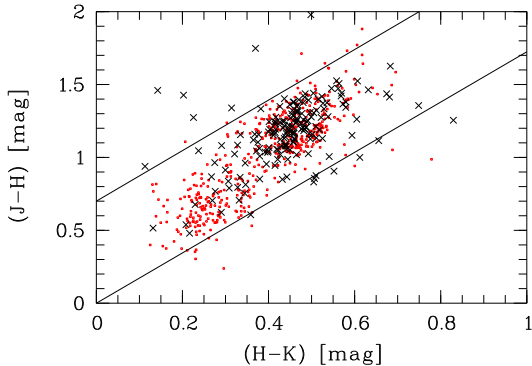


Figure 3. Colour-colour diagram of stars closer than $43''$ (crosses) and a control field of stars with distances of more than $100''$ to the cluster centre (dots). The solid lines represent the reddening path, i.e. they envelope the region in which main sequence and giant stars are situated.

field of view. We note that no point source is detected in the MSX images in the area of the cluster.

To determine the extinction along the line of sight to the cluster, we selected only stars closer than $43''$ from the cluster centre. In this case only a few stars show low reddening values, i.e. they are foreground objects. The majority of objects shows similar colours as the giant stars in the control field. We determine the mean colour excess of those stars compared to the control field as: $\langle H - K \rangle = 0.24$ mag, $\langle J - H \rangle = 0.58$ mag, $\langle J - K \rangle = 0.74$ mag. Using a standard powerlaw for the extinction $A_\lambda \propto \lambda^{-\beta}$ with $\beta = 1.8$ (Draine (2003)), we can directly compute the reddening in the K-band. We obtain $A_K = 0.38$ mag, 0.55 mag, and 0.44 mag for the $\langle H - K \rangle$, $\langle J - K \rangle$, and $\langle J - H \rangle$ colour excess values, respectively. Note that other extinction laws (i.e. $\beta = 1.6$ or using Fitzpatrick (1999)) result in slightly larger values for A_K . Hence in the following we will use a reddening for the cluster of $A_K = 0.5 \pm 0.1$ mag. Note that the uncertainty in A_K includes any possible reddening of the field stars whose colours are basically coincident with an unreddened population (Bessel & Brett (1988)).

3.3 Distance

To determine the distance to the cluster we need to identify objects of known absolute magnitudes. Due to the metallicity of $[M/H] = -0.8 \pm 0.1$ (Sect. 3.4) the locus of stars in the post-He-flash phase of evolution, i.e. the horizontal branch (HB) is expected to be degenerated to a clump of stars close to the red giant branch (RGB). Additionally, one can use the stars in the RGB bump, which are pre-He-flash objects. For the absolute magnitudes of these objects, considering our metallicities, we find $M_K^{\text{RGB bump}} = -1.5 \pm 0.1$ mag from Valenti et al. (2004) for old globular clusters. For the HB stars we find $M_K^{\text{HB}} = -1.4 \pm 0.1$ for a 6 Gyr and -1.2 ± 0.1 mag for a 12 Gyr old population (Salaris & Girardi (2002)). Hence, the signals produced by these two features in the luminosity function are not widely separated where the HB is expected to provide a stronger signal (see e.g. the infrared colour magnitude diagrams of old clusters given by Ferraro et al. (2000)).

Figure 4 shows a histogram of the apparent K-band magnitudes of all stars less than $43''$ from the cluster centre, and in a colour range $0.3 < (H - K) < 0.7$. We can compare this to the histogram of objects outside a $100''$ radius (normalised to the cluster area). In Fig. 4 one can see that above $m_K = 12$ mag there are

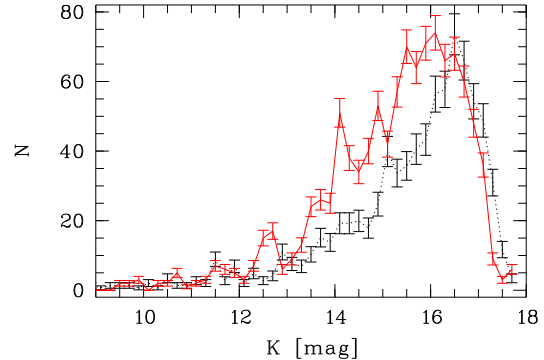


Figure 4. Histogram of the apparent K-band magnitude of stars closer than $43''$ to the cluster centre (solid line) and outside a radius of $100''$ (dotted line), normalised to the same area.

more stars in the cluster than in the control area. Due to the lower completeness limit in the cluster, above $m_K = 16.5$ mag the number of stars in the cluster drops below the number in the control field. The histogram of the cluster stars shows a significant peak at $m_K = 14.1$ mag which we interpret as the HB stars. We note that this peak appears in the histogram independent of the binning used. The peak at about $m_K = 15$ mag disappears when using different bin sizes. There is another peak at $m_K = 12.6$ mag, which is also significant. It is 0.4 mag wide and about 1.5 mag brighter than the HB. Alves et al. (2002) found a similar bump for stars in the Large Magellanic Cloud and interpreted it as the AGB bump of stars that are at the onset of helium shell burning. The brightness difference of 5.5 mag between the tip of the RGB and the $m_K = 14.1$ mag peak further supports our interpretation that the latter represents the HB.

Given the absolute magnitudes for the HB stars, we can estimate an extinction corrected distance modulus of $m - M = 15.0 \pm 0.2$ or 14.8 ± 0.2 mag for a 6 and 12 Gyr old population, respectively. This corresponds to a distance from the Sun of 10.0 ± 1.0 or 9.1 ± 1.0 kpc. With the Galactocentric distance of 8.5 kpc for the Sun, the Galactocentric distance of the cluster is $R_{GC} = 3.6 \pm 0.6$ or 3.2 ± 0.6 kpc. The distance to the Galactic plane is $z = -320$ or -290 pc, and the cluster core diameter is 2.3 or 2.1 pc.

3.4 Metallicity

One can follow Valenti et al. (2004) to determine the metallicity $[M/H]$ of the cluster. This requires to measure the slope of the RGB stars in the K vs. (J-K) diagram. Only stars brighter than the HB/RGB bump should be used. In Fig. 5 we show the (J-K) vs. K colour-magnitude diagram. Stars between $100''$ and $110''$ away from the cluster centre (control field) are plotted in the right panel. In the left panel squares indicate all stars within $43''$ from the cluster centre. We mark with triangles the stars that were used to obtain the best fit (solid line). Depending on which stars exactly we choose to determine the fit, we obtain a range from $-0.09 \dots -0.08$ for the slope in the diagram. According to Fig. 8 in Valenti et al. (2004), this converts into the metallicity range $-0.7 < [M/H] < -0.9$.

3.5 Integrated Brightness

To determine the brightness of the entire cluster, we can use two approaches. a) Integrate the flux from all stars in the area of the cluster, and correct statistically for foreground/background stars using

the histogram in Fig. 4. b) Integrate all the flux in the cluster area and correct by the average flux outside the cluster. Method a) hence determines the integral brightness of all detected stars, while b) determines the integral light of all stars in the cluster. The integrated apparent K-band brightness (corrected for A_K) of all detected stars in the cluster is $m_K^{stars}=8.1$ mag. When determining the integral dereddened brightness of the entire flux we obtain $m_K^{all}=6.6$ mag. This shows that only 25 % of the flux from the cluster is in the detected stars. The rest is in the unresolved cluster population. If all the undetected stars were as bright as the extinction corrected completeness limit in the cluster (i.e. $m_K=15.2$) then we are missing about 2800 stars. Together with the estimated 300 members brighter than $m_K=14.7$ mag (see Sect. 3) the cluster has a minimum number of 3100 member stars. This is, however, a weak lower limit, since it does not account for the stars between $m_K=14.7$ and 15.7 and the fact that the unresolved population is certainly dominated by stars fainter than $m_K=15.7$ mag. An independent estimate of the total number of stars will be discussed in Sect. 4.3.

With the distance modulus we can convert the apparent dereddened K-band magnitude of the integrated light ($m_K^{all}=6.6$ mag) into an absolute magnitude of $M_K = -8.2 \pm 0.2$ mag (assuming a 12 Gyr old population). This can be converted into $M_V = -6.3$ mag using $V - K = 1.9 \pm 0.1$ mag (Leitherer et al. (1999)).

4 CLASSIFICATION

In the following we will discuss the three possibilities for the classification of FSR 1735: 1) young open cluster, 2) old open cluster, 3) globular cluster.

4.1 Young open cluster

To classify Cl 1715 as a young stellar cluster it should show signs of on-going or recent star formation. It is at the same line of sight as a faint cloud of dust seen in emission in the MSX Band A image. However, the cloud is much more extended than the cluster, and the entire area is covered with faint emission patches in the MSX Band A image. Furthermore, there is no bright emission at far infrared wavelengths visible at the cluster position in the IRAS images. This indicates that the dust cloud is foreground to the cluster, and indeed to most of the other field stars. This fact is also supported by the apparent gap in the colour-colour diagram (see Fig. 3). Hence, there is no definite indication that the dust cloud is physically connected to the cluster.

There are no MSX or IRAS point sources in the cluster indicating on-going star formation. In the colour-colour diagram in Fig. 3 there are 11 objects below the reddening path, which might indicate that these are young stellar objects. This number is higher than what is expected from the control field. About 1-2 stars per cluster area in the control field are below the reddening path. We have hence checked all 11 YSO candidates by eye in order to verify their colour. All but one object turn out to be close double stars and/or very faint with problems in the photometry. The reason might be that the SExtractor software has problems with faint stars in crowded regions of variable background brightness (this effect accounts as well for the objects above the reddening path). Hence, only one object remains below the reddening path. Note that a slight change in the assumed dust properties of the reddening material can bring almost all of the YSO candidates into the reddening path as well.

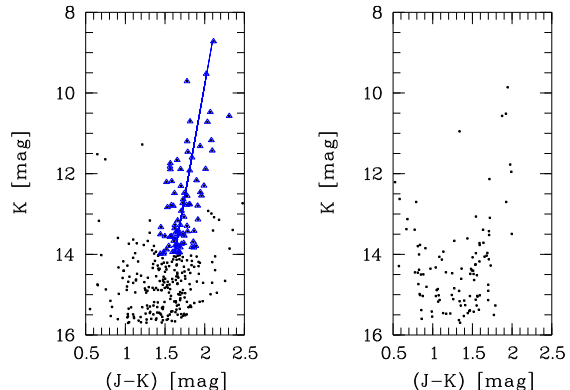


Figure 5. (J-K) vs. K colour-magnitude diagram of stars closer than 43'' from the cluster centre (left) and a control field of stars between 100'' and 110'' away from the cluster centre (right). The triangles in the left panel mark all stars brighter than the HB that were used to fit the slope of the RGB. The best fit is shown as a solid line.

There is also no radio continuum source connected to the cluster, which could be indicating on-going star formation. The closest radio source in the 4.85 GHz survey of Wright et al. (1994) is a 48 ± 9 mJy detection 4.35' from the cluster centre.

The cluster is situated close to the Galactic Plane. However, at the computed distance of 9.1 kpc it would be 290 pc below the plane, which is about 5.5 times the scale height of 53 ± 5 pc for open clusters (Joshi et al. (2005)). Hence, the position of the cluster in the inner Galaxy in combination with its sub-solar metallicity of $[M/H] = -0.8$ is also a strong argument against the interpretation of FSR 1735 as a young open cluster.

4.2 Old open cluster

If there are no signs of on-going star formation the object could be an old open cluster. However, the position in the Galaxy poses a strong argument against this interpretation. As shown a 6 Gyr old population would have a Galactocentric distance of 3.6 kpc and is situated 320 pc below the Galactic plane. While the distance to the plane is in agreement with the scale-height of 375 pc for old open clusters determined by Janes & Phelps (1994), the distance to the Galactic centre is too low to interpret FSR 1735 as an old open cluster. According to Friel (1995), old Galactic clusters are totally absent inside 7.5 kpc from the Galactic centre. This is caused by frequent encounters with giant molecular clouds in the inner Galaxy that destroy such objects. Note, that even if the peak at $m_K = 12.6$ mag is the HB, the Galactocentric distance of the cluster would be only 4.2 kpc.

If it is an old open cluster outside the 7.5 kpc radius, a distance of about 15 kpc would be required. Given our reddening and $[M/H]$ values, this is only possible for an at maximum 0.5 Gyr old population (Salaris & Girardi (2002)), i.e. $M_K^{HB} = -2.3$ mag. It is, however, questionable how such a low metallicity cluster can have formed only 500 Myrs ago at this Galactocentric distance. One furthermore expects a number of luminous supergiants $M_K < -6$ for such a young population. Only one such object is found. It is thus very improbable that the object is an old open cluster.

Table 1. Measured properties of the cluster FSR 1735 (assuming a 12 Gyr population). Listed are the right ascension, declination, Galactic longitude, Galactic latitude, K-band extinction, metallicity, core radius, tidal radius, central star density, distance to the Sun, distance to the Galactic centre, distance to the Galactic plane, diameter, absolute K-band magnitude and the cluster mass.

Parameter	Value
R.A. (J2000)	16 52 10.6
DEC (J2000)	−47 03 29
l [deg]	339.1879
b [deg]	−1.8534
A_K [mag]	0.5 ± 0.1
[M/H]	-0.8 ± 0.1
R_{core} ["]	23.5
R_{tid} ["]	86
I_{cen} [*/arcsec ²]	0.27
R_{\odot} [kpc]	9.1 ± 1.0
R_{GC} [kpc]	3.2 ± 0.6
z_{GP} [pc]	290
d [pc]	2.1
M_K [mag]	-8.2 ± 0.2
$M_{cluster}$ [M_{\odot}]	65000

4.3 Globular cluster

Does FSR 1735 resemble a typical GC? According to Salaris & Girardi (2002) a 12 Gyr old population has $4.7 \cdot 10^{-4}$ HB stars per solar mass of originally formed stars. From the star counts we estimate about 30 HB stars in FSR 1735 which yields a cluster mass estimate of $6.5 \cdot 10^4 M_{\odot}$. Assuming an average mass of $0.5 M_{\odot}$ per star, this converts into $\sim 10^5$ stars in the cluster. Hence, every determined cluster parameter (summarised in Table 1) as well as the objects position in the Galaxy supports the interpretation of FSR 1735 as a so far unknown Milky Way globular cluster.

All parameter values are well within the typical range of the known GCs in the Galaxy (e.g. Harris (1996)). Hence, the object could be one of the about 10 missing globular clusters in the inner part of the Galaxy (Ivanov et al. (2005)). The circular optical appearance of the cluster further supports this interpretation. However, to accurately determine the cluster position in the Galaxy and the other parameters we need to measure the age. This is not possible with the currently available dataset and requires much deeper observation down to the cluster main sequence.

5 CONCLUSIONS

We present the new Milky Way globular cluster candidate FSR 1735 from a 2MASS-based near infrared cluster search (Froeblich et al. (2006)). The analysis is based on deep JHK images taken with Sofi at the NTT. The images show a rich circular cluster of stars. Radial star density profiles show that the more luminous stars ($R_{core}=23.5''$) are more concentrated towards the cluster centre than the fainter stars ($R_{core}=41.5''$). This can be explained by magnitude migration due to crowding. The reddening to the cluster is estimated to $A_K=0.5 \pm 0.1$ mag, mostly caused by a single cloud of gas and dust in the line of sight. From (J-K) vs. K colour magnitude diagrams we determine a metallicity of $[M/H]=-0.8 \pm 0.1$.

The significant peak in the K-band luminosity function of the cluster is interpreted as the clump of horizontal branch stars. Based on this we estimate a distance for the object of 9.1 ± 1.0 kpc, an absolute brightness of $M_K = -8.2 \pm 0.2$ mag and a diameter of

2.1 pc. The number of horizontal branch stars is used to estimate a cluster mass of about $6.5 \cdot 10^4 M_{\odot}$.

The lack of indications of on-going or recent star formation in the cluster (no YSOs, IRAS or MSX sources, radio continuum sources) lets us to conclude that the object is not a young open cluster. The position in the Galaxy, i.e. the Galactocentric distance, poses strong arguments against the interpretation of FSR 1735 as an old open cluster. Only an at maximum 0.5 Gyr old open cluster with $[M/H]=-0.8$ could explain the observations, which would be, however, clearly at variance with the age-metallicity relation for the Galactic disc.

All the available observational evidence is in agreement with the interpretation that FSR 1735 is a so far unknown globular cluster in the inner Milky Way. A definite determination of the object parameters, however, requires to measure the age of the cluster accurately, which is not possible with the currently available dataset.

ACKNOWLEDGMENTS

We would like to thank the referee Sergio Ortolani for helpful comments.

REFERENCES

- Alves, D.R., Rejkuba, M., Minniti, D., Cook, K.H. ApJ, 573, 51
 Bertin, E., Arnouts, S. 1996, A&AS, 117, 393
 Bessell, M.S., Brett, J.M. 1988, PASP, 100, 1134
 Bica, E., Dutra, C.M., Soares, J., Barbuy, B. 2003, A&A, 404, 223
 Carraro, G. 2005, ApJ, 621, 61
 Carpenter, J.M., Heyer, M.H., Snell, R.L. 2000, ApJS, 130, 381
 Draine, B.T. 2003, ARA&A, 41, 241
 Dutra, C.M., Bica, E. 2000, A&A, 359, 9
 Dutra, C.M., Bica, E. 2001, A&A, 376, 434
 Ferraro, F.R., Montegriffo P., Origlia, L. & Fusi Pecci, F. 2000, AJ, 119, 1282
 Fitzpatrick, E.L. 1999, PASP, 111, 63
 Friel, E.D. 1995, ARA&A, 33, 381
 Froeblich, D., Scholz, A., Raftery, C.L. 2006, MNRAS, 374, 399
 Harris, W.E. 1996, AJ, 112, 1487
 Hurt, R.L., Jarrett, T.H., Kirkpatrick, J.D., Cutri, R.M., Schneider, S.E., Skrutskie, M., van Driel, W. 2000, AJ, 120, 1876
 Ivanov, V.D., Borissova, J., Pessev, P., Ivanov, G.R., Kurtev, R. 2002, A&A, 394, 1
 Ivanov, V.D., Kurtev, R., Borissova, J. 2005, A&A, 442, 195
 Janes, K.A., Phelps, R.L. 1994, AJ, 108, 1773
 Joshi, Y.C. 2005, MNRAS, 362, 1259
 Koblinsky, H.A., Monson, A.J., Buckalew, B.A., et al. 2005, AJ, 129, 239
 Kronberger, M., Teutsch, P., Alessi, B., et al. 2006, A&A, 447, 921
 Leitherer, C., Schaerer, D., Goldader, J.D., et al. 1999, ApJS, 123, 3
 Marshall, D.J., Robin, A.C., Reylé, C., Schultheis, M., Picaud, S. 2006, A&A, 453, 635
 Mathis, J.S. 1990, ARA&A, 28, 37
 Ortolani, S., Bica, E., Barbuy, B. 2000, A&A, 361, 57
 Salaris, M., Girardi, L. 2002, MNRAS, 337, 332
 Skrutskie, M.F., Cutri, R.M., Stiening, R., et al. 2006, AJ, 131, 1163

6 *Froebrich, Meusinger & Scholz*

Valenti, E., Ferraro, F. R., Perina, S., Origlia, L. 2004, *A&A*, 419, 139

Willman, B., Blanton, M.R., West, A.A., et al. 2005, *AJ*, 129, 2692

Wright, A.E., Griffith, M.R., Burke, B.F., Ekers, R.D. 1994, *ApJS*, 91, 111